Shifting velocity of temperature extremes under climate change

Joan Rey[1,2], Guillaume Rohat[2,3,4], Marjorie Perroud[2], Stéphane Goyette[1,2], Jérôme Kasparian[1,2]

[1] Group of Applied Physics, University of Geneva, Chemin de Pinchat 22, 1211 Geneva 4, Switzerland

[2] Institute for Environmental Sciences, University of Geneva, blvd Carl Vogt 66, 1211 Geneva 4, Switzerland

[3] Faculty of Geo-Information Science and Earth Observation, University of Twente, 7514 AE Enschede, The Netherlands

[4] National Center for Atmospheric Research (NCAR), 80301 Boulder, CO, United-States

E-mail: `jerome.kasparian@unige.ch`

17 April 2019

Abstract. Rapid changes in climatic conditions threaten both socioeconomic and ecological systems, as these might not be able to adapt or to migrate at the same pace as that of global warming. In particular, an increase of weather and climate extremes can lead to increased stress on human and natural systems, and a tendency for serious adverse effects. Relying on the EURO-CORDEX simulations, we compare the shifting velocities of cold and hot extremes of the screen-level daily mean temperature (T2m), with that of the associated central trends, *i.e.*, the arithmetical mean or median. Defining the extremes relative to the T2m distribution as it evolves in time over the period of 1950–2100, we find that temperature extremes shift at a velocity similar to that of the central trends. Indeed, the T2m probability distribution shifts as a whole, as the tails of the distribution increase together with the central trends. Exceptions however occur in specific regions and for the clustering of warm days, which shifts slower than all other extremes investigated in this study.

1. Introduction

Global warming is arguably one of the most pressing contemporary societal issues, leading to changes in both global and local climatic conditions that directly affect a number of natural and anthropogenic systems worldwide [1]. There is a vivid demand from stakeholders, decision makers, and other practitioners for climate change projections in view of both mitigation and adaptation strategies [2]. Such information is required at various spatial and temporal scales, from local to global and from the near-yearly to centennial perspectives.

The adaptation window for both ecological and human systems is highly dependent on the pace of climate change. When the focus is on the local adaptation of ecosystems, industrial process or organizational changes, such a speed is locally defined using the temporal derivative of the considered climatic variables. However, when adaptation implies migration of species, shifts of biota, or relocation of human settlements and activities, spatial aspects of the climate shift are crucial. Two different approaches have been employed so far to explore the potential impacts of such spatial aspects on various socio-economic activities, such as forestry [3], agriculture [4, 5], and urban planning [6, 7].

On the one hand, climate analogues (or "climate twins") [8, 9, 10] are well-suited to raise awareness of decision makers and lay audience about the speed and magnitude of climate change, as they convey an easy-to-understand message by comparing climatic conditions at well-identified places and times. Climate analogues are areas that are expected to experience, at a given time-period, the climate of a reference location at another time period. Dividing the distances between the two paired locations by the considered time interval defines a shifting velocity of climate [11, 10]. This approach allows to consider multiple variables, such as temperature and precipitation [12] or purpose-specific climate indices, *e.g.* bio-climatic indices [5, 13]. It also accounts for natural barriers such as mountainous regions or marine areas. Furthermore, it helps identifying climates that are expected to disappear in the future, or future emerging conditions not encountered to date – *i.e.* those that have no future or past analogues [14, 15]. However, the shifting velocity may depend on the matching scheme and parametrization, and can be overestimated [16, 17].

To avoid this overestimation and to identify the speed of climate displacement regardless of natural barriers, one can alternatively focus on the shifting velocity of climate through the displacement of isopleths, *e.g.*, isotherms if the focus is on temperature. Such shifting velocity can be defined as the displacement vector, per unit of time, of the local climatic conditions characterized by the isopleth(s) corresponding to the considered variable(s) [18]. This is generally achieved at the cost of implicit assumptions, as detailed and discussed below. Within this framework, a system can keep pace with a moving climate if its maximum shifting velocity is at least comparable to that of the relevant climatic parameters [18].

Among all climate-related phenomena, extreme temperature events [19] have a wide

range of impacts on anthropic and natural systems. In many cases, they affect both directly and indirectly human health and well-being [20]. Examples include increasing heat-related illness and casualties [21, 22, 23], power failures, degradation of critical infrastructure during heat waves [24], reduced crop yields [25, 23], and economic loss – *e.g.* due to reduced labour hours, extreme events-related costs, or increased health care needs [26]. The expected impact of climate extremes is made even more important by the projections that some of these extreme events will become more frequent, more widespread, longer, and/or more intense during the XXIst Century [1, 27, 28, 29, 30]. New insights about the spatial and temporal shift of temperature extremes could help assess the effect of climate change on the spatial behavior, occurrence, and distribution of these extremes, to better assess the future state of ecosystems (*e.g.* [31, 32, 33, 34, 35]) and to anticipate impacts and required adaptation measures for human populations and systems (*e.g.* [6, 7, 8, 9, 11, 36]).

Here we quantify the spatial shift of temperature extremes and compare their velocity to that of the corresponding central trends. We focus on screen-level air temperature (T2m) over the European Coordinated Downscaling Experiment (EURO-CORDEX) domain [37], for the period 1951–2100. We consider the climate scenario according to the Representative Concentration Pathway (RCP) 8.5 [38]. Under this high greenhouse gas emission scenario, the increase in mean land T2m ranges from 2.5 to 5.5 °C over Europe by 2081–2100 relative to 1986–2005 [39].

Up to 27 different definitions of extreme temperature events have been proposed by the World Meteorological Organization [40, 41, 42, 43]. We focus on several of them: the tails of the probability distribution function (PDF) (high/low quantiles or standard deviations), the exceedance of fixed thresholds (tropical nights or frost days), and the clustering of warm days, in an approach similar to warm spells [44].

We find that, overall, temperature extremes and the corresponding central trends shift across Europe with a similar velocity. This applies to extremes defined relative to the PDF tails as well as to a fixed threshold. In contrast, the clustering of successive warm days shifts much slower than the central trend. We also identify and discuss the few regions where the shifting velocity of the temperature extremes deviates from that of the central trends. Finally, we show that the similarity of shifting velocities between extremes and central trends is closely related to the definition of new normals [45].

2. Methods

2.1. Datasets

This work relies on climate data from high-resolution (0.11°) regional climate models (RCMs) simulated within the EURO-CORDEX [37] initiative for the period 1951–2100 for the RCP 8.5 scenario [38]. The domain spans between the following geographical coordinates: (63.55°N, 51.56°W), (63.65°N, 72.56°E), (20.98°N, 14.31°W), and (20.98°N, 72.56°E). The ability of EURO-CORDEX simulations to reproduce

present-day temperature extremes has been demonstrated (*e.g.* [46, 47]) and their outputs have been widely used to analyze projections of extreme temperatures in Europe (*e.g.* [48]). We use historical runs for the period 1951–2005 and projections for 2006–2100. Our analysis primarily relies on ALADIN-5.3 (hereafter named ALADIN), a RCM developed by Météo-France [49, 50]. To assess the robustness of our findings against the choice of this particular RCM, we replicate the analysis with three other RCM outputs, namely HIRHAM 5 (HIRAM, DMI [51]), RACMO-22E (RACMO, KNMI [52]), and REMO2009 (REMO, MPI [53]).

2.2. Climate variables

We base the analysis on the screen-level air temperature and consider its daily mean (T2m), minimum (T2m,min), and maximum (T2m,max).

We first compare the evolution of the annual median of T2m to that of the cold (percentiles 1, 2, 5, 10, and 20) and hot (percentiles 80, 90, 95, 98, and 99) quantiles of the annual and seasonal PDF of T2m. Consistent with the approach of the new normals [45], we consider the PDF as it evolves as a function of time rather than the historical PDF.

Alternatively, we compare the evolution of the yearly averaged T2m with that of the values at $\pm 0.5\sigma$, $\pm 1\sigma$, $\pm 1.5\sigma$, and $\pm 2\sigma$, σ being the yearly standard deviation of the daily T2m values. If T2m were to follow a Gaussian distribution, these thresholds would correspond to percentiles 30 and 70, 16 and 84, 6 and 94, and 2 and 98, respectively. We also consider the number of tropical nights (T2m,min $\geq 20\,^{\circ}\mathrm{C}$) and the number of frost days (T2m,max $\leq 0\,^{\circ}\mathrm{C}$) [40]. Finally, we define a *warm days clustering index* (WDCI) as the total number of days that belong to a sequence of at least three consecutive days with a daily-averaged T2m above the percentile 90 of the local annual T2m PDF. In order to account for the temporal evolution of the PDF with respect to global warming, we detrend the PDF by substracting a 30-year linear regression fit. Tropical nights, frost days, and clustered warm days occur in a limited number each year (e.g, WDCI $\leq 35\,\mathrm{yr}^{-1}$ according to the above definition). To achieve statistical significance, we bin their yearly counts into 30-years periods (1951–1980, 1981–2010, 2011–2040, 2041–2070, and 2071-2100).

2.3. Evaluation of the shifting velocity

A so-called index of the velocity of temperature change has first been proposed by Loarie *et al.* [18]. Here, we detail further this approach, its mathematical foundations, and we explicitly describe and discuss the underlying assumptions. The calculation of shifting velocities relies on the well-known relation between the Eulerian (or partial) and Lagrangian (or particulate) derivatives [54] of a value ψ along the trajectory of an arbitrary point moving at velocity $\vec{v}$:

$$\frac{\mathrm{d}\psi}{\mathrm{d}t} = \frac{\partial\psi}{\partial t} + \vec{v}\cdot\vec{\nabla}\psi. \tag{1}$$

In the present work, ψ may represent the yearly median or mean of T2m, the quantiles of the yearly T2m distribution, or the values at $\pm\lambda\sigma$, λ being a positive real number. It may also be the numbers of tropical nights, of frost days, or the WDCI, binned over 30-years periods.

By definition of an isopleth, for any point shifting with an iso-ψ line, the Lagrangian derivative is $\frac{\mathrm{d}\psi}{\mathrm{d}t} = 0$, so that

$$\frac{\partial\psi}{\partial t} = -\vec{v}\cdot\vec{\nabla}\psi. \tag{2}$$

To solve this equation and determine $\vec{v}$, a second relationship between $\vec{v}$ and $\vec{\nabla}\psi$ is required. In that purpose, we assume that the iso-ψ lines (*e.g.*, isotherms if ψ is temperature, or isochrones if ψ represents a duration in terms of number of days) shift over time down the gradient of ψ. Their velocity is therefore oriented opposite to the unit vector $\vec{u}_\nabla$ pointing along the gradient of ψ (*i.e.* $\vec{u}_\nabla = \frac{\vec{\nabla}\psi}{||\vec{\nabla}\psi||}$). This assumption implies that isopleths shift parallel to each other without significant deformation, and that their curvature can locally be neglected. Under this assumption, the shifting velocity vector expresses as:

$$\vec{v} = -\frac{1}{||\vec{\nabla}\psi||}\frac{\partial\psi}{\partial t}\vec{u}_\nabla. \tag{3}$$

The magnitude of the local shifting velocity $v = ||\vec{v}||$ of the isopleth, is then:

$$v = \frac{1}{||\vec{\nabla}\psi||}\frac{\partial\psi}{\partial t}. \tag{4}$$

Equation (3) averages over time to:

$$\overline{\vec{v}} = -\overline{\frac{1}{||\vec{\nabla}\psi||}\frac{\partial\psi}{\partial t}\vec{u}_\nabla}. \tag{5}$$

The assumption that the isopleths shift down the gradient, parallel to each other and without deformation implies that the covariance between temporal fluctuations of the terms lying on the right hand side of Equation (5) is neglected. As the gradient is orthogonal to the isopleths, this assumption also implies that $\vec{u}_\nabla$ is constant, so that $\overline{\vec{u}_\nabla} = \vec{u}_\nabla$ and Equation (5) rewrites:

$$\overline{\vec{v}} = -\frac{1}{\left|\left|\overline{\vec{\nabla}\psi}\right|\right|}\overline{\left(\frac{\partial\psi}{\partial t}\right)}\,\vec{u}_\nabla. \tag{6}$$

As a result, the magnitude of the average shifting velocity vector over the considered time period, hereafter denoted the *shifting velocity*, expresses as:

$$\overline{v} = \frac{1}{\left|\left|\overline{\vec{\nabla}\psi}\right|\right|}\overline{\left(\frac{\partial\psi}{\partial t}\right)}. \tag{7}$$

At each grid point, the temporal average of the partial derivative $\overline{\left(\frac{\partial\psi}{\partial t}\right)}$ is determined as the slope of a linear regression over 1951–2100, and the gradient is calculated with centered differences.

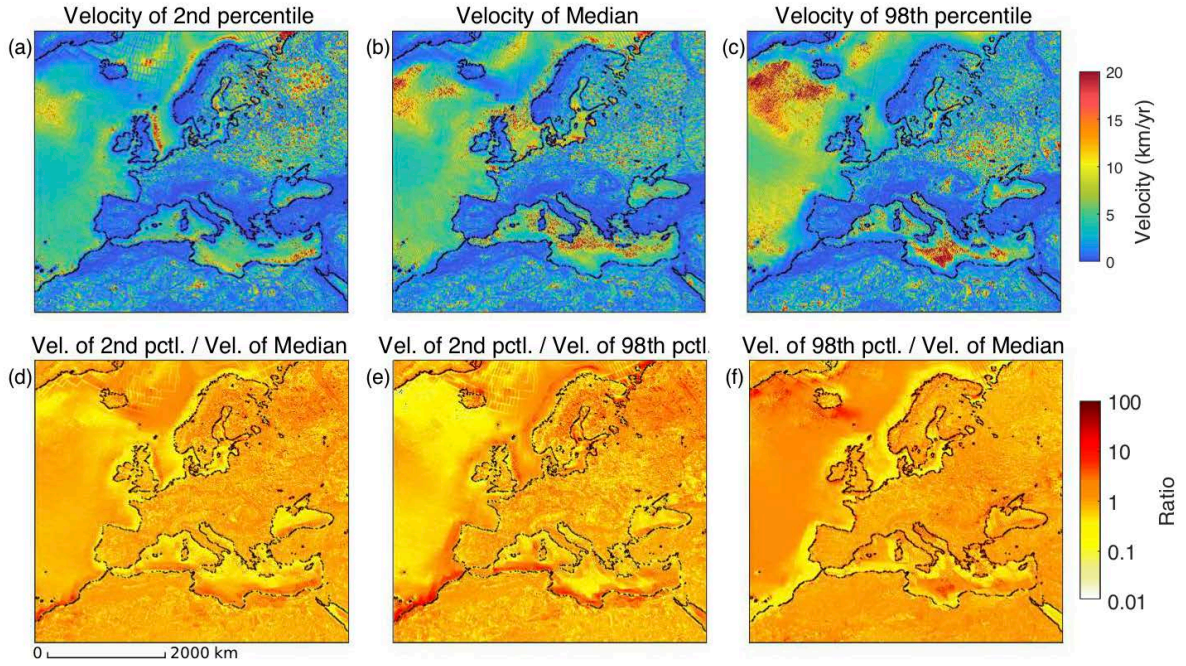

Figure 1. (a–c) Shifting velocities averaged over 150 years (1951–2100) of percentiles 2 (low extremes, a) 50(median, b) and 98 (hot extremes, c) of the daily T2m. (d–f) Ratio of these velocities: (d) percentile 2 to median; (e) percentile 2 to percentile 98; (f) percentile 98 to median.

3. Results

3.1. Median and extreme quantiles

Figure 1b displays the shifting velocity of the yearly median for T2m. The isotherms of the annual median T2m shifts faster over most marine areas, as expected from previous works (*e.g.* [55]). This is especially true over the Atlantic Ocean and the Mediterranean Sea. Faster shifting velocities are also found across Western Russia. Conversely, the median of T2m shifts slower over mountainous regions such as the Alps, the Atlas, as well as in Scandinavia. These fast (resp. slow) shifting velocities correspond to smoother (resp. steeper) gradients (Figure S1b), while the temperature change is quite homogeneous over the considered time period (Figure S1e).

The shifting velocity of hot and cold extremes, represented by the percentiles 2 and 98 respectively (Figure 1a,c), show spatial patterns and magnitudes similar to those of the median, but differ at specific locations. The cold extremes shift slower than the median over the Atlantic Ocean West of Iceland, and the Eastern part of the Mediterranean Sea. In contrast, they shift faster than the median on the East coast of Great Britain and Northern Russia. Conversely, the hot extremes move faster in the Central Mediterranean Sea and the Northern Atlantic Ocean – particularly West of Iceland –, and slower on the West coast of the North Sea and Northern Russia. These behaviors appear to be governed more by the differences in the gradient steepness

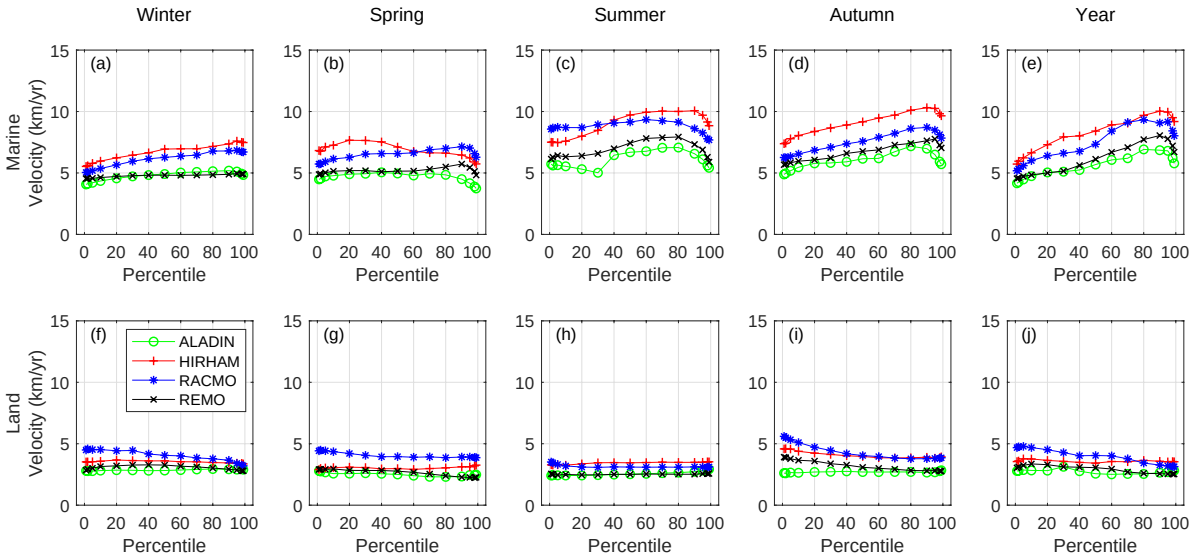

Figure 2. Mean shifting velocities as a function of the quantiles, averaged over marine regions (a–e) and land (f–j), for Winter (DJF, a and f), Spring (MAM, b and g), Summer (JJA, c and i), Fall (SON, d and j), and for the yearly mean (e and k). Data are computed by four RCMs between 1951 and 2100

(Figure S1a,c) than by the local temporal evolution (Figure S1d,f) of cold and hot extremes.

The ratio between the shifting velocities of percentiles 2, 50, and 98 (Figure 1d–f) evidence further details pertaining to coastal regions. Off the coasts of Western Europe and in the North-Eastern Mediterranean Sea, both cold and hot extremes shift significantly slower than the median. In contrast, off the North coast of Africa, both in the Atlantic Ocean and the Southern Mediterranean Sea, the cold extremes shift faster than the median, while the hot extremes shift slower.

Figure 2 displays the shifting velocity as a function of the quantile. The rather homogeneous velocities described above translate in very flat dependences. This results in an overall shifting of the T2m PDF, with little deformation on both land and marine regions (Figure 3).

Three alternative climate models (HIRHAM, RACMO, and REMO) yield similar trends as ALADIN in spite of local quantitative differences in the shifting velocities (Figure S2). In particular, the shifting velocity increases with quantiles in all models in the Mediterranean Sea and the Atlantic Ocean especially West of Iceland. Also, the median shifts faster than both extremes in the North Sea and the Sea of Norway in the four models. In contrast, the decrease of the shifting velocity with the quantile over Russia is much stronger in RACMO than in ALADIN, and smaller in REMO and HIRHAM. While multi-model ensemble simulations would increase the accuracy and the delineation of uncertainty ranges [56], the similarity of the results across models indicates that relying on a single model is sufficient for the purpose of this study.

Figure 4 displays the two-dimensional histograms relating the shifting velocities

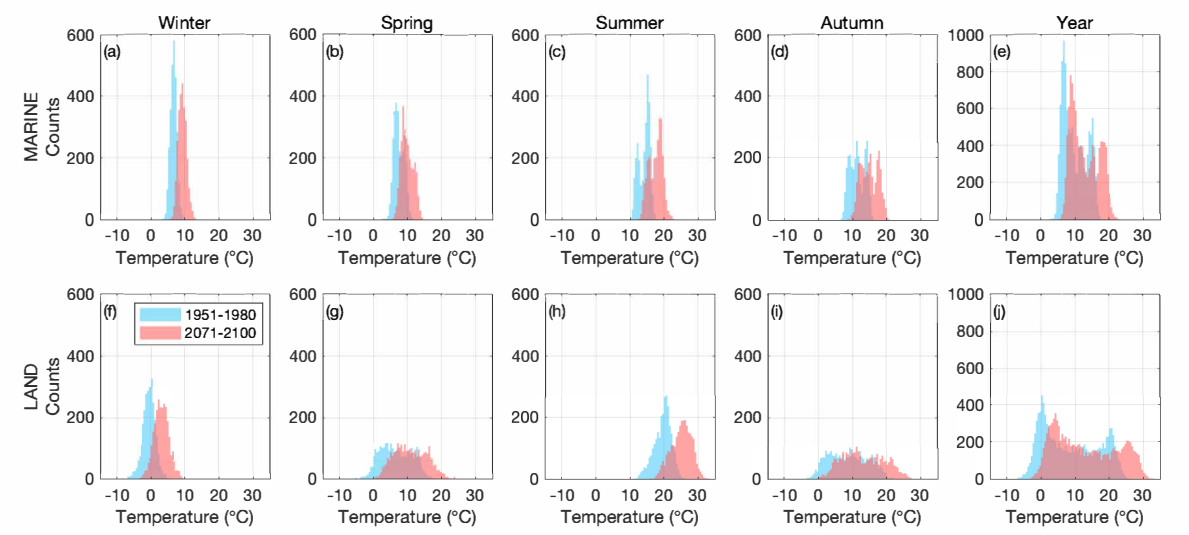

Figure 3. Evolution of the probability distribution functions of the daily mean T2m between 1951–1980 and 2071–2100, over marine regions (a–e) and over land (f–j), in Winter (DJF, a and f), Spring (MAM, b and g), Summer (JJA, c and i), Fall (SON, d and j), and for the whole year (e and k); the vertical scale of the latter has been adapted for clarity.

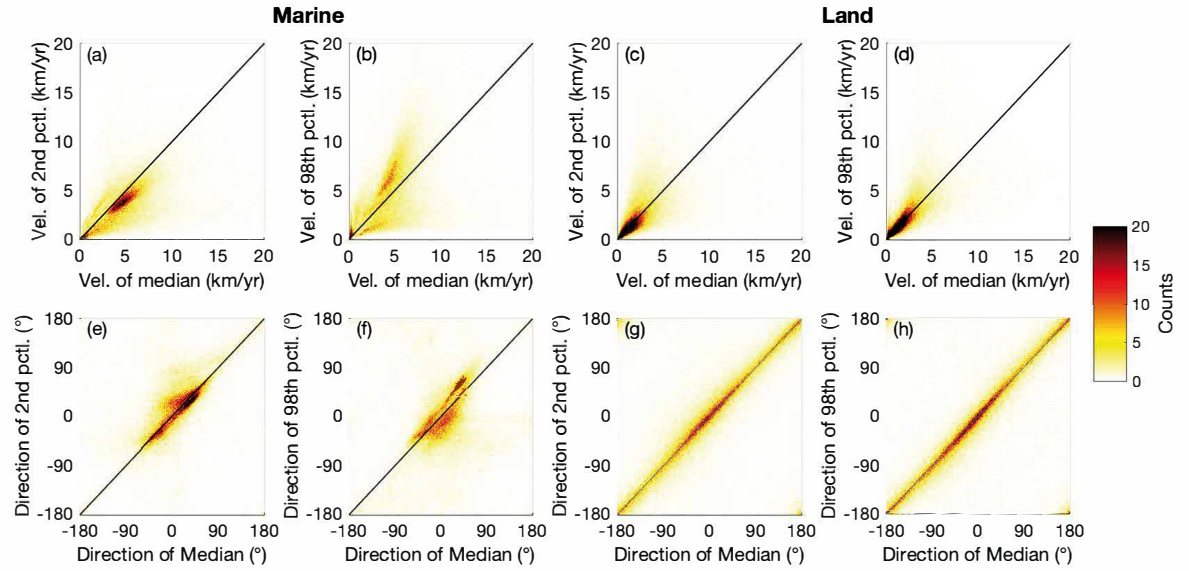

Figure 4. Two-dimensional histograms of the distributions of the shifting velocities of T2m percentiles in Europe, over marine regions (a,b,e,f) and over land (c,d,g,h), between 1951 and 2100. Velocity magnitude (a–d) and direction (e–h) of percentiles 2 (a,c,e,g) and 98 (b,d,f,h), with respect to the median. Directions 0°, 90°, ±180°, −90° respectively refer to northward, eastward, southward and westward.

of the median to that of the extreme percentiles; Panels a–d focus on the velocity magnitude, while panels e–h display the shifting directions. The similarity of the shifting velocities of the median and the extreme percentiles, as discussed above (Figure 1), is also evidenced on these two-dimensional histograms, particularly over land where both

magnitudes (Figure 4c,d) and directions (Figure 4g,h) cluster along the diagonal.

Over marine regions, shifting velocities are slightly more dispersed. The percentiles 2 (Figure 4a) and 98 (Figure 4b) respectively display marginally slower and faster shifts than the median, consistent with the results showed in Figure 1. For cold extremes (Panel a), the stripe deviating down from the diagonal corresponds to coastal regions and to the Atlantic Ocean West of Iceland. Regarding hot extremes (Panel b), the stripe above the diagonal corresponds to the Atlantic Ocean. In spite of these small fluctuations, the overall shifting directions of the extreme percentiles and the median over marine regions are rather similar, although slightly more spread than those over land.

The same analysis has been carried out by considering the percentiles 1 (resp. 99), 5 (95), and 10 (90) instead of 2 (98) as the cold (hot) extremes. Similar results are found, although the features described above are slightly stronger for more extreme percentiles. We also performed the same analysis with the annual mean as the central value, and $\pm 0.5\sigma$, $\pm\sigma$, $\pm 1.5\sigma$, or $\pm 2\sigma$ of the T2m, as the temperature extremes (Figures S3 to S5 for $\pm 2\sigma$). The results are very similar with each other and with those obtained considering quantiles and the median. This can be understood by considering that the yearly median and the mean of the daily T2m are extremely correlated, both in space ($R \geq 0.99$) and in time ($R \geq 0.999$). Their difference is limited to $\pm 0.5\,^{\circ}\mathrm{C}$ over almost 70% of the grid cells.

Therefore, the behavior of the shifting velocity of the temperature extremes defined with respect to the T2m PDF is to a large extent immune to the particular definition of the extremes. This immunity covers the choice of the central trend (median or mean), the tails of the distribution (percentiles or standard deviations), as well as the cutoff chosen in the temperature distribution to define the extremes. This corroborates the robustness of our findings.

3.2. Tropical nights, frost days, and warm days clustering

As displayed on Figure 5, isochrones defining the number of tropical nights per year generally shift much faster over marine regions, as well as over Russia and Northern Africa (Figure 5a). This behavior is similar to that of the median (Figure 1b), in spite of a slightly faster shifting velocity. As a result, the ratio between the corresponding velocities is quite homogeneous, with an average value of 1.08 over all regions where it is defined (Figure 5d). The slightly faster shifting velocity of the tropical nights as compared with the T2m median is also evidenced by a deviation of data above the diagonal in the two-dimensional histograms of Figure 6a. The only exceptions are the Atlantic Ocean off the Spanish coast and the Black Sea located at the Southeastern extremity of Europe, where the tropical night isochrones locally shift up to 2–6 times faster than the median. In spite of these deviations, the shifting direction of the tropical night isochrones is comparable to that of the T2m median (Figure 6d). The dispersion of shifting directions mostly corresponds to the rounding errors related to low shifting

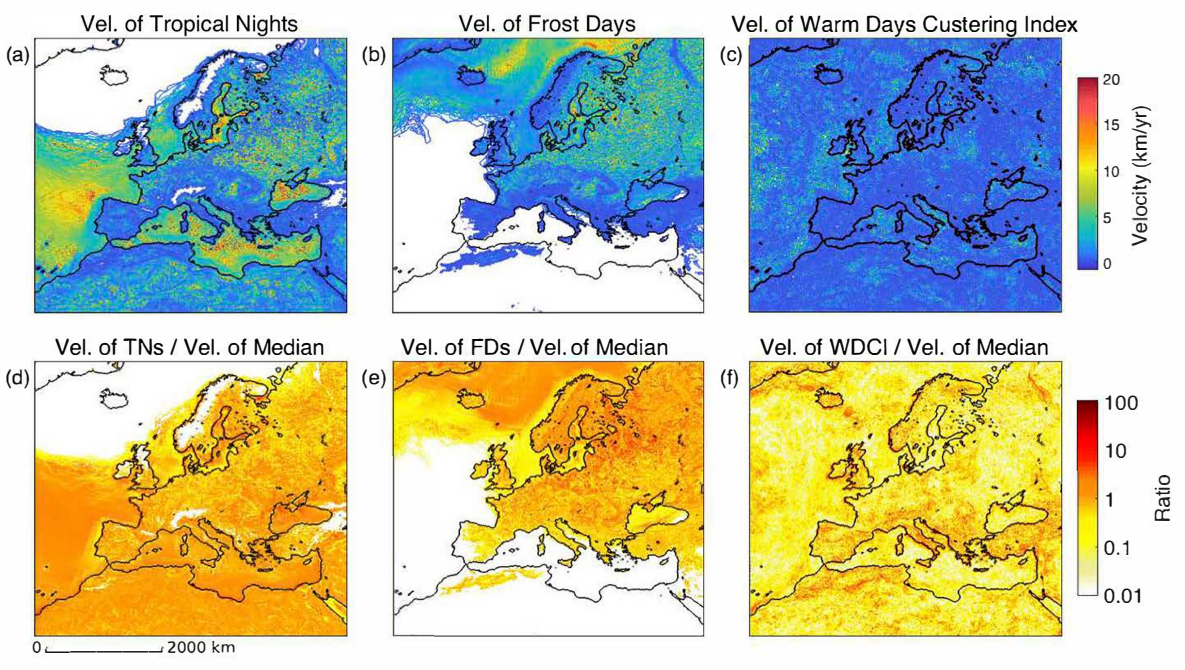

Figure 5. (a,b,c) Shifting velocity of the occurrence frequency of (a) tropical nights (TNs), (b) frost days (FDs), and (c) Warm days clustering index (WDCI). (d–f) Corresponding ratio to the shifting velocity of the median T2m. Sub-regions free of the considered situations are displayed in white.

velocities.

Where they occur, the isochrones corresponding to the number of frost days also shift at velocity magnitudes and directions comparable to that of the median (Figure 5b, Figure 6b,e) over most of the domain. However, they shift slower than the median in both the North Sea and in the Atlantic Ocean South of Iceland (Figure 5e).

Finally, the WDCI shifts typically 4 times slower (1 km/year) over the whole domain than the T2m median as well as than the other extremes investigated in this study (Figure 5c,Figure 5f and Figure 6c). Slightly faster shifts are however observed over the Atlantic Ocean (1.73 km/year on average) and to a lesser extent over Russia (1.2 km/year on average).

4. Discussion

The results reported above show no systematic differences, neither in direction nor in magnitude, between shifting velocities of the central temperature trend, and that of the extremes. This is especially true over land and with regard to the extremes defined relative to the temperature PDF. This can be understood by considering that the temperature PDF turns out to be to a large extent spatially homogeneous, and that its shape barely evolves as it shifts with global warming.

This study also shows that the shifting velocity conveys complementary information as compared to the local temperature evolution. In Scandinavia, Northern Russia, and

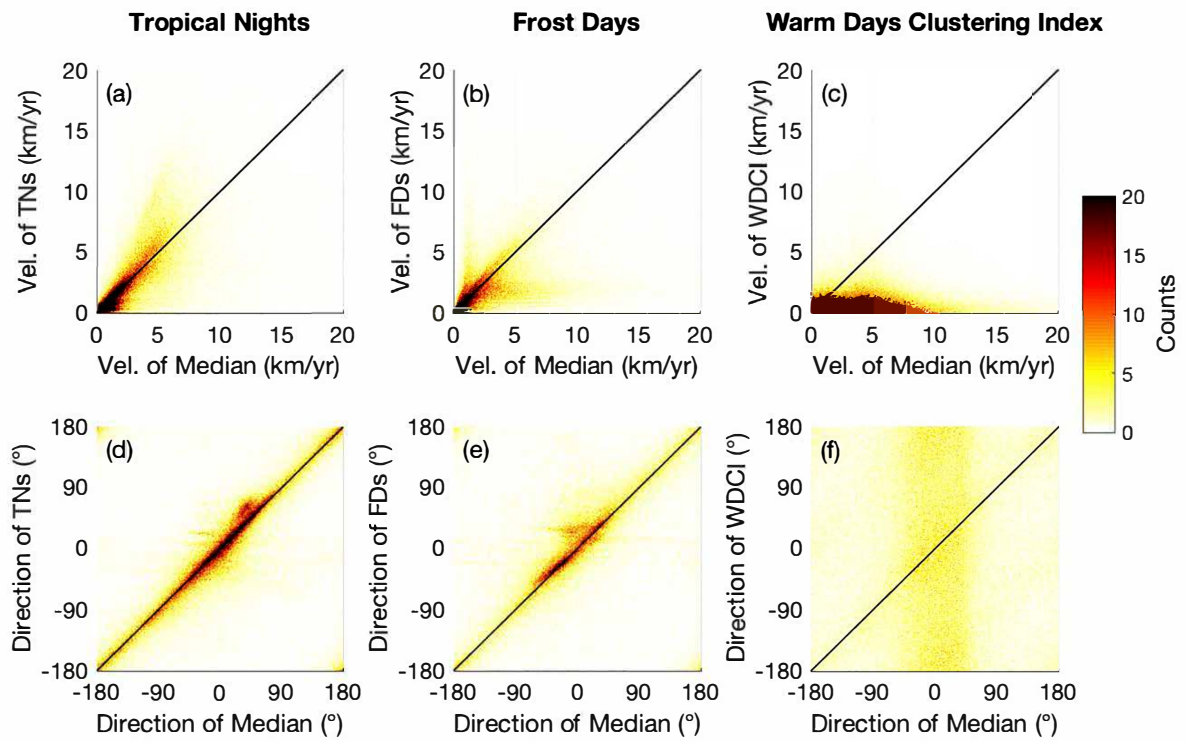

Figure 6. Two-dimensional histograms of (a–c) the magnitude and (d–f) direction of the shifting velocities of (a,d) tropical nights, (b,e) frost days, and (c,f) WDCI compared to the median T2m, over the period 1951–2100. Directions 0°, 90°, ±180°, −90° respectively refer to northward, eastward, southward and westward.

offshore from them, the cold extremes increase much faster than hot ones (Figure S1d,f). However, as their gradient is also steeper (Figure S1a,c), this does not translate into faster shifting velocities. The steep gradient can be related to the edge of the sea-ice or snow cover. Ice and snow keep the cold extremes below the freezing point. Conversely, ocean and land surfaces are much less reflective to solar radiation, ensuing positive ice-snow albedo feedbacks [57]. As a consequence, displacements of the edge of the ice or snow cover locally allows the cold extreme to rise beyond zero, resulting in a fast local rise of cold extremes.

The finding that temperature extremes and the central trend generally shift at a similar velocity could appear to contradict previous studies, which found extremes to actually increase faster than the central trends [28, 29, 30]. This apparent paradox is related to the definition of the extremes. Here we consider extremes as the tails of the temperature PDF *during each time period*, while most existing studies define extremes with regards to the historical (*e.g.*, the 1990s) PDF. As the PDF shifts as a whole, an increasing number of climatic conditions falls into the definition of extremes relative to today's or past PDF. They however become new normals [45] since their values approach the new central ones. In other words, today's hot extremes would become increasingly frequent, but also increasingly "normal", *i.e.*, less and less extreme from a statistical point of view. In that sense, today's extremes draw an idea of tomorrow's central trends,

but under such a definition, extremes will not become more frequent in the future.

Temperature extremes defined with reference to absolute thresholds also generally shift as a whole at a comparable velocity as the central trends, again with local exceptions. Indeed, one may note that T2m,min and T2m,max shift at a same velocity as the T2m itself (Figure S6; See also Figure 1b), *i.e.*, the daily thermal amplitude does not increase with climate warming. Consequently, the threshold conditions also shifts together with the central trend.

Only the WDCI displays a shifting velocity significantly different (and much slower) from that of the median T2m and the other indicators investigated in this work. The reason for this is that WDCI represents a metric of the clustering of the number of days with T2m in the hottest decile. The yearly number of days in the hottest decile is constant by definition. The very slow average shifting velocity (1 km/yr) of the WDCI isochrones simply means that these hot days cluster only marginally more, except over the Atlantic Ocean.

5. Conclusion

Measuring the velocity of climate change represents a substantial scientific challenge. In this paper, we calculate the shifting velocities of central trends and extremes of screen-level air temperature, using EURO-CORDEX RCM simulations between 1951 and 2100, according to the RCP8.5 emission scenario. We find that T2m extremes shift at a comparable speed as the central trends over Europe, except over a limited number of sub-regions. This somewhat unexpected result can be explained on the basis of the T2m PDFs that generally shift as a whole with minimal deformations. Consequently, today's extreme situations would, to a large extent, become new normals by the end of the XXIst Century. While current hot extremes will become more and more frequent, these situations will not be deemed extreme anymore in a warmer climate. Similarly, cold extremes will not disappear under climate warming, but they will correspond to less and less cold events as the normals warms up.

Research suggests that biodiversity adaptability to increased temperatures is somewhat limited and that their first response to changing climatic conditions is a shift in location [58], with migration patterns often being slower than changes in climatic conditions [59]. Overall, human adaptability to temperature extremes has been increasing over the past decades [60, 61], but further research is needed to compare the speed of human adaptability with that of climate shift and to characterize context-specific limits of human adaptability [62, 63].

Further assessments regarding shifting velocities should be carried out by taking into account the deformation of isotherms during their displacements, and investigating the role of processes like soil moisture, snow and sea-ice modifications and related surface-atmosphere feedbacks.

Acknowledgments. We gratefully acknowledge technical support by Roman Kanala at the Institute for Environmental Sciences. The EURO-CORDEX data used in

this study were obtained from the Earth System Grid Federation server (https://esgf-data.dkrz.de/projects/esgf-dkrz/). We thank all the modeling groups that performed the simulations and made their data available.

6. References

[1] IPCC 2014 *Climate change 2014: Impacts, Adaptation and Vulnerability. Contribution of the Working Group II to the Fifth Assessment Report of the Intergovernmental Panel on Climate Change* (Cambridge, UK, and New-York, NY, USA: Cambridge University Press)

[2] Hewitt C, Mason S and Walland D 2012 *Nature Climate Change* **2** 831 URL https://doi.org/10.1038/nclimate1745

[3] Leibing C, Signer J, Van Zonneveld M, Jarvis A and Dvorak W 2013 *Forests* **4** ISSN 1999-4907

[4] Webb L B, Watterson I, Bhend J, Whetton P H and Barlow E W R 2013 *Australian Journal of Grape and Wine Research* **19** 331–341 ISSN 1322-7130 URL https://doi.org/10.1111/ajgw.12045

[5] Ramírez-Villegas J, Lau C, Köhler A K, Signer J, Jarvis A, Arnell N, Osborne T and Hooker J 2011 Climate analogues: finding tomorrow's agriculture today Report CGIAR Research Program on Climate Change, Agriculture and Food Security (CCAFS)

[6] Rohat G, Goyette S and Flacke J 2017 *Mitigation and Adaptation Strategies for Global Change* **22** 929–945 ISSN 1573-1596 URL https://doi.org/10.1007/s11027-016-9708-x

[7] Hallegatte S, Hourcade J C and Ambrosi P 2007 *Climatic Change* **82** 47–60 ISSN 1573-1480 URL https://doi.org/10.1007/s10584-006-9161-z

[8] Ungar J, Peters-Anders J and Loibl W 2011 Climate twins – an attempt to quantify climatological similarities *Environmental Software Systems. Frameworks of eEnvironment* ed Hřebíček J, Schimak G and Denzer R (Springer Berlin Heidelberg) pp 428–436 ISBN 978-3-642-22285-6

[9] Kopf S, Minh H D and Hallegatte S 2008 Using maps of city analogues to display and interpret climate change scenarios and their uncertainty Report URL http://inis.iaea.org/search/search.aspx?orig_q=RN:41023434

[10] Beniston M 2014 *International Journal of Climatology* **34** 1838–1844 ISSN 0899-8418 URL https://doi.org/10.1002/joc.3804

[11] Rohat G, Goyette S and Flacke J 2018 *International Journal of Climate Change Strategies and Management* **10** 428–452 ISSN 1756-8692 URL https://www.emeraldinsight.com/doi/abs/10.1108/IJCCSM-05-2017-0108

[12] Dahinden F, Fischer E M and Knutti R 2017 *Environmental Research Letters* **12** 084004 ISSN 1748-9326 URL http://dx.doi.org/10.1088/1748-9326/aa75d7

[13] Littlefield C E, McRae B H, Michalak J L, Lawler J J and Carroll C 2017 *Conservation Biology* **31** 1397–1408 ISSN 0888-8892 URL https://doi.org/10.1111/cobi.12938

[14] Saxon E, Baker B, Hargrove W, Hoffman F and Zganjar C 2005 *Ecology Letters* **8** 53–60 ISSN 1461-023X URL https://doi.org/10.1111/j.1461-0248.2004.00694.x

[15] Williams J W and Jackson S T 2007 *Frontiers in Ecology and the Environment* **5** 475–482 ISSN 1540-9295 URL https://doi.org/10.1890/070037

[16] Carroll C, Lawler J J, Roberts D R and Hamann A 2015 *PLOS ONE* **10** e0140486 URL https://doi.org/10.1371/journal.pone.0140486

[17] Hamann A, Roberts D R, Barber Q E, Carroll C and Nielsen S E 2015 *Global Change Biology* **21** 997–1004 ISSN 1354-1013 URL https://doi.org/10.1111/gcb.12736

[18] Loarie S R, Duffy P B, Hamilton H, Asner G P, Field C B and Ackerly D D 2009 *Nature* **462** 1052 URL https://doi.org/10.1038/nature08649

[19] Alexander L V, Zhang X, Peterson T C, Caesar J, Gleason B, Klein Tank A M G, Haylock M, Collins D, Trewin B, Rahimzadeh F, Tagipour A, Rupa Kumar K, Revadekar J, Griffiths G, Vincent L, Stephenson D B, Burn J, Aguilar E, Brunet M, Taylor M, New M, Zhai P, Rusticucci

M and Vazquez-Aguirre J L 2006 *Journal of Geophysical Research: Atmospheres* **111** ISSN 0148-0227 URL https://doi.org/10.1029/2005JD006290

[20] Vasseur David A, DeLong John P, Gilbert B, Greig Hamish S, Harley Christopher D G, McCann Kevin S, Savage V, Tunney Tyler D and O'Connor Mary I 2014 *Proceedings of the Royal Society B: Biological Sciences* **281** 20132612 URL https://doi.org/10.1098/rspb.2013.2612

[21] Bell J E, Brown C L, Conlon K, Herring S, Kunkel K E, Lawrimore J, Luber G, Schreck C, Smith A and Uejio C 2018 *Journal of the Air & Waste Management Association* **68** 265–287 ISSN 1096-2247 URL https://doi.org/10.1080/10962247.2017.1401017

[22] Royé D 2017 *International Journal of Biometeorology* **61** 2127–2140 ISSN 1432-1254 URL https://doi.org/10.1007/s00484-017-1416-z

[23] FAO 2018 Fao's work on climate change - united nations climate change conference 2018 Report Food and Agriculture Organization of the United Nations

[24] McEvoy D, Ahmed I and Mullett J 2012 *Local Environment* **17** 783–796 ISSN 1354-9839 URL https://doi.org/10.1080/13549839.2012.678320

[25] Liu Q, Piao S, Janssens I A, Fu Y, Peng S, Lian X, Ciais P, Myneni R B, Peñuelas J and Wang T 2018 *Nature Communications* **9** 426 ISSN 2041-1723 URL https://doi.org/10.1038/s41467-017-02690-y

[26] Hsiang S, Kopp R, Jina A, Rising J, Delgado M, Mohan S, Rasmussen D J, Muir-Wood R, Wilson P, Oppenheimer M, Larsen K and Houser T 2017 *Science* **356** 1362 URL http://science.sciencemag.org/content/356/6345/1362.abstract

[27] IPCC 2012 *Managing the risks of extreme events and disasters to advance climate change adaptation. A special report of working groups I and II of the Intergouvernmental Panel on Climate Change.* (Cambridge, UK, and New-York, NY, USA.: Cambridge University Press)

[28] Lewis S C and King A D 2017 *Weather and Climate Extremes* **15** 1–10 ISSN 2212-0947 URL http://www.sciencedirect.com/science/article/pii/S2212094716300512

[29] Lewis S C, King A D and Mitchell D M 2017 *Geophysical Research Letters* **44** 9947–9956 ISSN 0094-8276 URL https://doi.org/10.1002/2017GL074612

[30] Horton R M, Coffel E D, Winter J M and Bader D A 2015 *Geophysical Research Letters* **42** 7722–7731 ISSN 0094-8276 URL https://doi.org/10.1002/2015GL064914

[31] Kelly A E and Goulden M L 2008 *Proceedings of the National Academy of Sciences* **105** 11823 URL http://www.pnas.org/content/105/33/11823.abstract

[32] Burrows M T, Schoeman D S, Richardson A J, Molinos J G, Hoffmann A, Buckley L B, Moore P J, Brown C J, Bruno J F, Duarte C M, Halpern B S, Hoegh-Guldberg O, Kappel C V, Kiessling W, O'Connor M I, Pandolfi J M, Parmesan C, Sydeman W J, Ferrier S, Williams K J and Poloczanska E S 2014 *Nature* **507** 492 URL https://doi.org/10.1038/nature12976

[33] García Molinos J, Halpern B, Schoeman D, Brown C, Kiessling W, Moore P, Pandolfi J, Poloczanska E, Richardson A and Burrows M 2015 *Nature Climate Change* **6** 83 URL https://doi.org/10.1038/nclimate2769

[34] Pinsky M L, Worm B, Fogarty M J, Sarmiento J L and Levin S A 2013 *Science* **341** 1239 URL http://science.sciencemag.org/content/341/6151/1239.abstract

[35] Dobrowski S Z, Abatzoglou J, Swanson A K, Greenberg J A, Mynsberge A R, Holden Z A and Schwartz M K 2013 *Global Change Biology* **19** 241–251 ISSN 1354-1013 URL https://doi.org/10.1111/gcb.12026

[36] Fitzpatrick M C and Dunn R R 2019 *Nature Communications* **10** 614 ISSN 2041-1723 URL https://doi.org/10.1038/s41467-019-08540-3

[37] Jacob D, Petersen J, Eggert B, Alias A, Christensen O B, Bouwer L M, Braun A, Colette A, Déqué M, Georgievski G, Georgopoulou E, Gobiet A, Menut L, Nikulin G, Haensler A, Hempelmann N, Jones C, Keuler K, Kovats S, Kröner N, Kotlarski S, Kriegsmann A, Martin E, van Meijgaard E, Moseley C, Pfeifer S, Preuschmann S, Radermacher C, Radtke K, Rechid D, Rounsevell M, Samuelsson P, Somot S, Soussana J F, Teichmann C, Valentini R, Vautard R, Weber B and Yiou P 2014 *Regional Environmental Change* **14** 563–578 ISSN 1436-378X URL

https://doi.org/10.1007/s10113-013-0499-2

[38] van Vuuren D P, Edmonds J, Kainuma M, Riahi K, Thomson A, Hibbard K, Hurtt G C, Kram T, Krey V, Lamarque J F, Masui T, Meinshausen M, Nakicenovic N, Smith S J and Rose S K 2011 *Climatic Change* **109** 5 ISSN 1573-1480 URL https://doi.org/10.1007/s10584-011-0148-z

[39] EEA 2018 Global and european temperature URL https://www.eea.europa.eu/data-and-maps/indicators/global-and-european-temperature-8/assessment

[40] ETCCDI 2001 Climate change indices: Definitions of the 27 core indices URL http://etccdi.pacificclimate.org/list_27_indices.shtml

[41] Karl T, Nicholls N and Ghazi A 1999 *Climatic Change* **42** 3–7

[42] Peterson T C, Folland C, Gruza G, Hogg W, Mokssit A and Plummer N 2001 Report on the activities of the working group on climate change detection and related rapporteurs Report World Meteorological Organization

[43] Peterson T C 2005 *World Meteorological Organization Bulletin* **54** 83–86

[44] French J, Kokoszka P, Stoev S and Hall L 2019 *Computational Statistics & Data Analysis* **131** 176–193 ISSN 0167-9473 URL http://www.sciencedirect.com/science/article/pii/S0167947318301701

[45] Lewis S C, King A D and Perkins-Kirkpatrick S E 2016 *Bulletin of the American Meteorological Society* **98** 1139–1151 ISSN 0003-0007 URL https://doi.org/10.1175/BAMS-D-16-0183.1

[46] Russo S, Sillmann J and Fischer E M 2015 *Environmental Research Letters* **10** 124003 ISSN 1748-9326

[47] Vautard R, Gobiet A, Jacob D, Belda M, Colette A, Déqué M, Fernandez J, Garcia-Diez M, Goergen K, Guttler I, Halenka T, Karacostas T, Katragkou E, Keuler K, Kotlarski S, Mayer S, van Meijgaard E, Nikulin G, Patarcic M, Scinocca J, Sobolowski S, Suklitsch M, Teichmann C, Warrach-Sagi K, Wulfmeyer V and Yiou P 2013 *Climate Dynamics* **41** 2555–2575

[48] Dosio A 2016 *Journal of Geophysical Research: Atmospheres* **121** 5488–5511 ISSN 2169-897X URL https://doi.org/10.1002/2015JD024411

[49] Colin J, Déqué M, Radu R and Somot S 2010 *Tellus A: Dynamic Meteorology and Oceanography* **62** 591–604 ISSN null URL https://doi.org/10.1111/j.1600-0870.2010.00467.x

[50] Herrmann M, Somot S, Calmanti S, Dubois C and Sevault F 2011 *Nat. Hazards Earth Syst. Sci.* **11** 1983–2001 ISSN 1684-9981 URL https://www.nat-hazards-earth-syst-sci.net/11/1983/2011/

[51] Christensen O B, Christensen J H, Machenhauer B and Botzet M 1998 *Journal of Climate* **11** 3204–3229 ISSN 0894-8755 URL https://doi.org/10.1175/1520-0442(1998)011<3204:VHRRCS>2.0.CO;2

[52] van Meijgaard E, van Ulft L, Lenderink G, De Roode S, Wipfler E, Boers R and van Timmermans R 2012 Refinement and application of a regional atmospheric model for climate scenario calculations of western europe Report Wageningen University and Research

[53] Jacob D, Elizalde A, Haensler A, Hagemann S, Kumar P, Podzun R, Rechid D, Remedio A R, Saeed F, Sieck K, Teichmann C and Wilhelm C 2012 *Atmosphere* **3** ISSN 2073-4433

[54] Sethian J A 2008 *Acta Numerica* **5** 309–395 ISSN 0962-4929 URL https://www.cambridge.org/core/article/theory-algorithms-and-applications-of-level-set-methods-for-propagating-interfaces/60DB748B21FE1A019ACABCC6FE40646A

[55] Burrows M T, Schoeman D S, Buckley L B, Moore P, Poloczanska E S, Brander K M, Brown C, Bruno J F, Duarte C M, Halpern B S, Holding J, Kappel C V, Kiessling W, O'Connor M I, Pandolfi J M, Parmesan C, Schwing F B, Sydeman W J and Richardson A J 2011 *Science* **334** 652 URL http://science.sciencemag.org/content/334/6056/652.abstract

[56] He W p, Zhao S s, Wu Q, Jiang Y d and Wan S 2019 *Climate Dynamics* **52** 2597–2612 ISSN 1432-0894 URL https://doi.org/10.1007/s00382-018-4410-1

[57] Robock A 1983 *Journal of the Atmospheric Sciences* **40** 986–997 ISSN 0022-4928 URL https://doi.org/10.1175/1520-0469(1983)040<0986:IASFAT>2.0.CO;2

[58] Pecl G T, Araújo M B, Bell J D, Blanchard J, Bonebrake T C, Chen I C, Clark T D, Colwell R K,

Danielsen F, Evengård B, Falconi L, Ferrier S, Frusher S, Garcia R A, Griffis R B, Hobday A J, Janion-Scheepers C, Jarzyna M A, Jennings S, Lenoir J, Linnetved H I, Martin V Y, McCormack P C, McDonald J, Mitchell N J, Mustonen T, Pandolfi J M, Pettorelli N, Popova E, Robinson S A, Scheffers B R, Shaw J D, Sorte C J B, Strugnell J M, Sunday J M, Tuanmu M N, Vergés A, Villanueva C, Wernberg T, Wapstra E and Williams S E 2017 *Science* **355** eaai9214 URL http://science.sciencemag.org/content/355/6332/eaai9214.abstract

[59] Renwick K M and Rocca M E 2015 *Global Ecology and Biogeography* **24** 44–51 ISSN 1466-822X URL https://doi.org/10.1111/geb.12240

[60] Sheridan S C and Allen M J 2018 *Environmental Research Letters* **13** 043001 ISSN 1748-9326 URL http://dx.doi.org/10.1088/1748-9326/aab214

[61] Sheridan S C and Dixon P G 2017 *Anthropocene* **20** 61–73 ISSN 2213-3054 URL http://www.sciencedirect.com/science/article/pii/S2213305416301096

[62] Pal J S and Eltahir E A B 2015 *Nature Climate Change* **6** 197 URL https://doi.org/10.1038/nclimate2833

[63] Sherwood S C and Huber M 2010 *Proceedings of the National Academy of Sciences* **107** 9552 URL http://www.pnas.org/content/107/21/9552.abstract

Supplementary Material

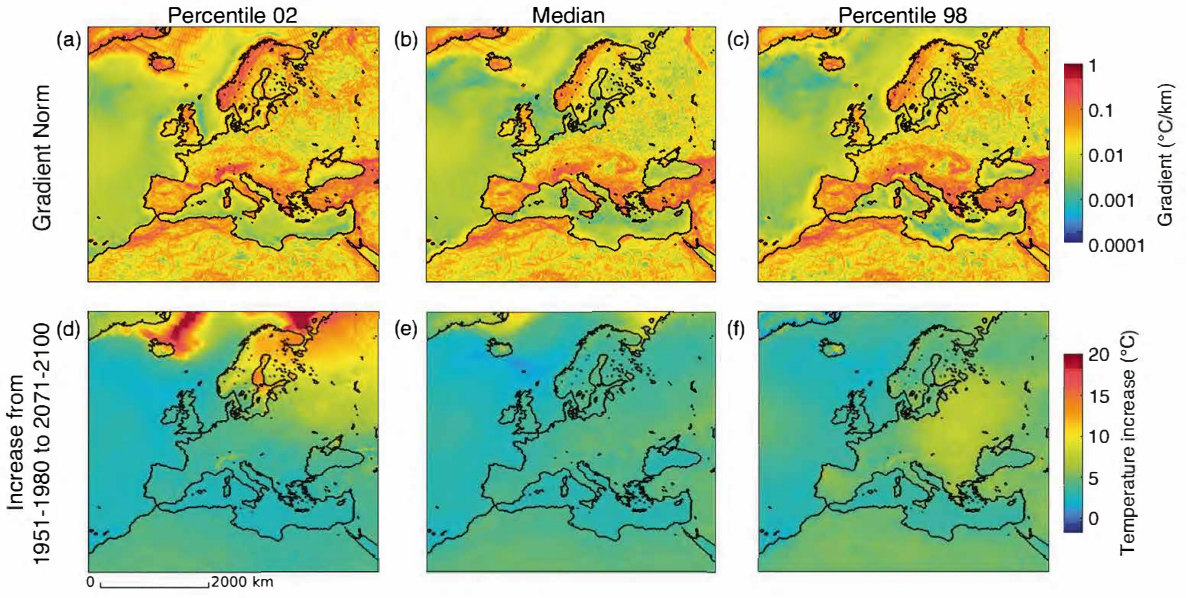

Figure S1. (a–c) Spatial gradients of T2m for percentiles 2 (a), 50 (b) and 98 (c), averaged over the period 1951–2100. (d–f) Evolution of percentiles 2 (d), 50 (e), and 98 (f) of the T2m PDF between the periods 1951–1980 and 2071–2100.

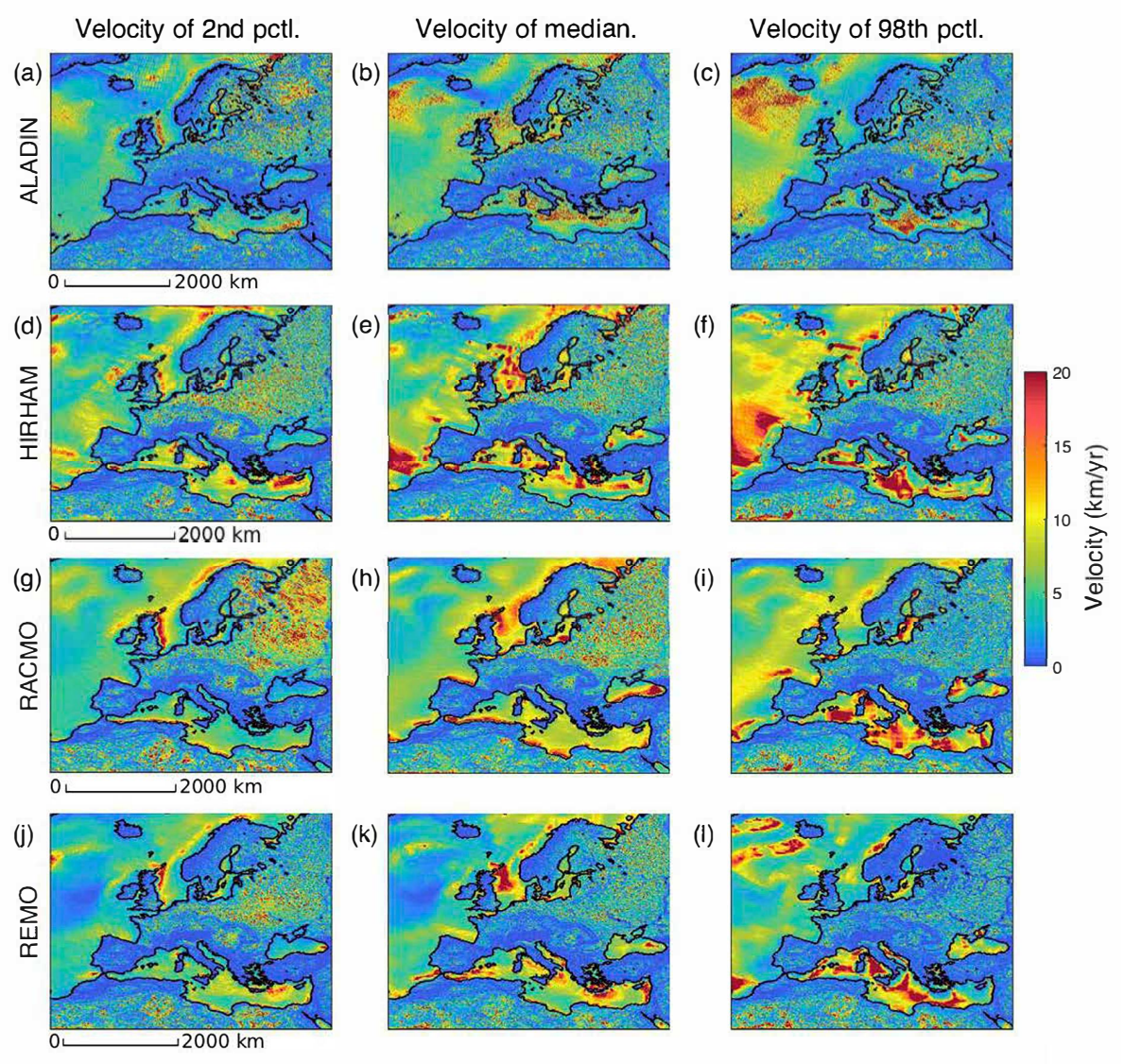

Figure S2. Shifting velocity over 150-year (1951–2100) of the daily T2m percentiles 2 (a,d,g,j), 50 (median, b,e,h,k) and 98 (c,f,j,l), for models ALADIN (from Figure 1, a–c), HIRAM (d–f), REMO (g–i), and RACMO (j–l).

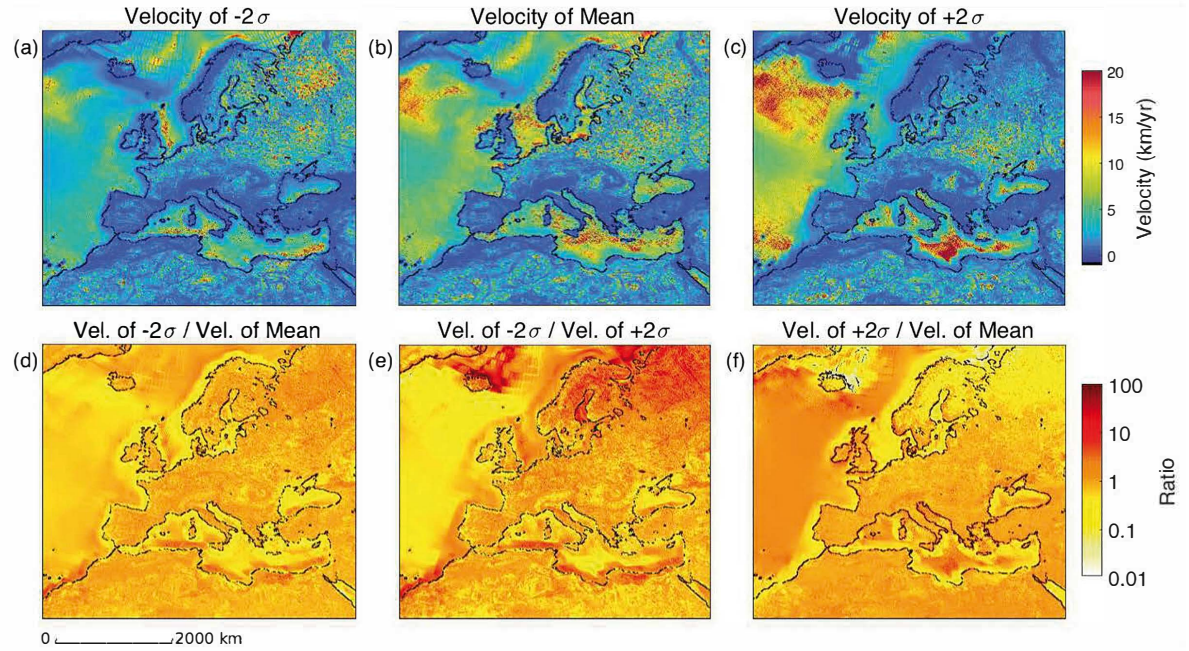

Figure S3. (a–c) Shifting velocity of the daily T2m mean (b) and values at -2σ (a) and $+2\sigma$ (c). (d–f) Ratio of these velocities. (d) -2σ to mean; (e) -2σ to $+2\sigma$ (f) $+2\sigma$ to mean.

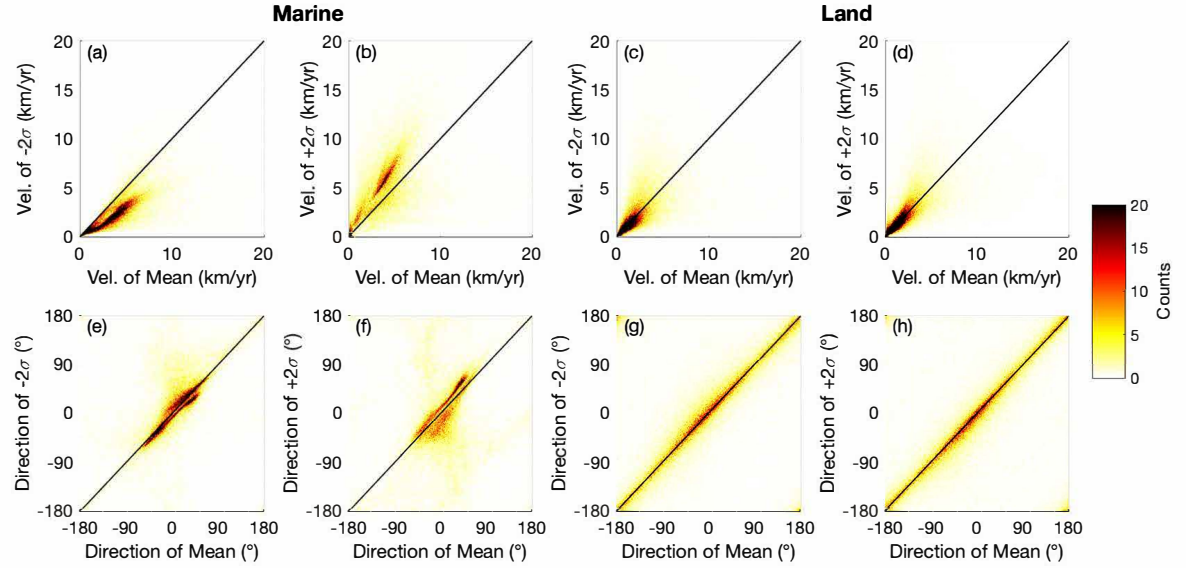

Figure S4. Two-dimensional histograms of the distributions of the shifting velocities of T2m mean and standard deviations in Europe, over marine regions (a,b,e,f) and over land (c,d,g,h), between 1951 and 2100. Velocity magnitude (a–d) and direction (e–h) of -2σ (a,c,e,g) and $+2\sigma$ (b,d,f,h), with respect to the mean. Directions 0°, 90°, ±180°, −90° respectively refer to northward, eastward, southward and westward.

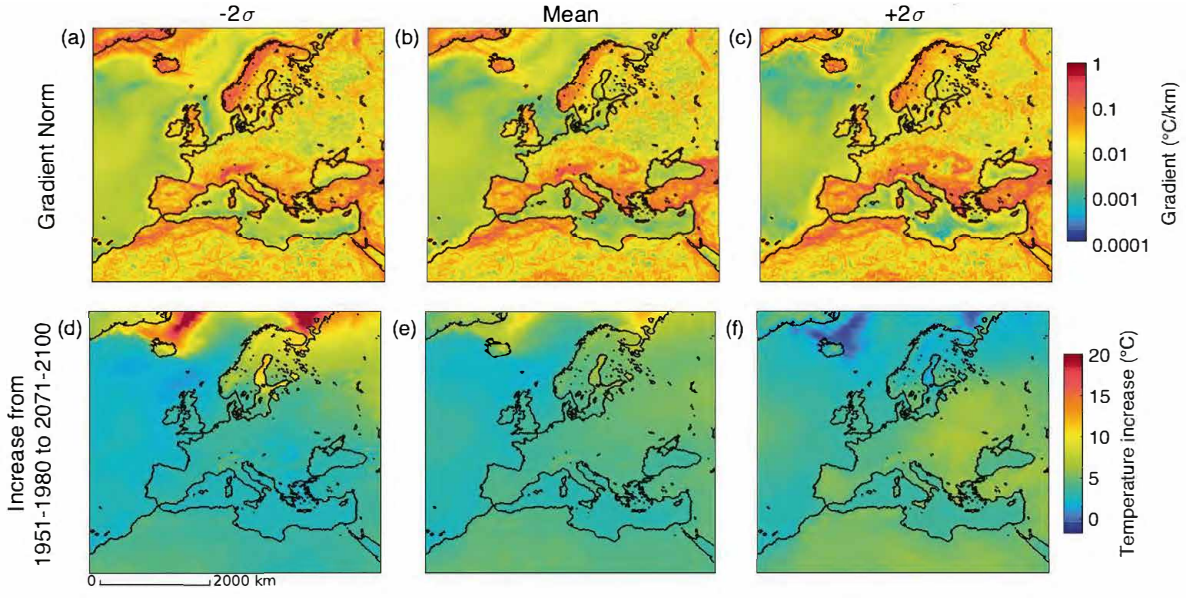

Figure S5. (a–c) Spatial gradients of T2m for -2σ (a), mean (b) and $+2\sigma$ (c), averaged over the period 1951–2100. (d–f) Evolution of -2σ (d), mean (e), and $+2\sigma$ (f) of the T2m PDF between the periods 1951–1980 and 2071–2100.

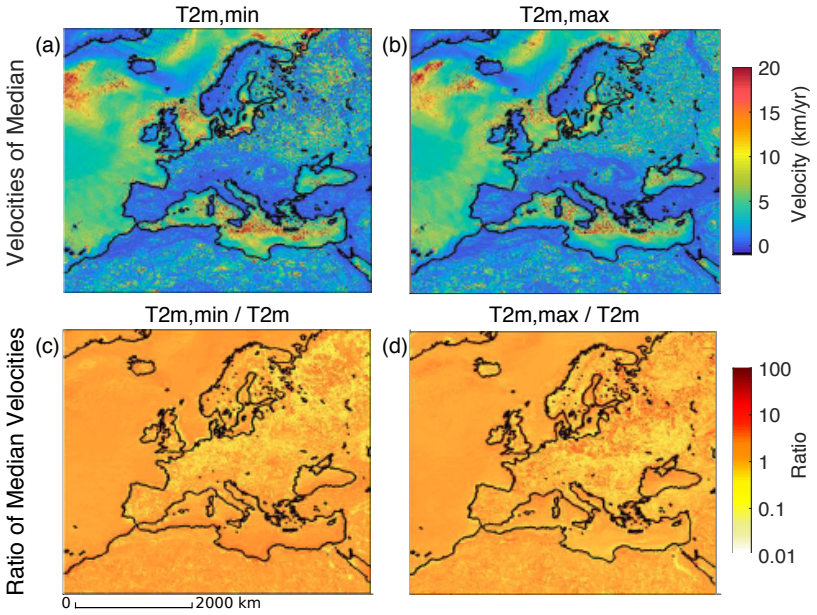

Figure S6. (a,b) Shifting velocity of the daily T2m,min (a) and T2m,max (b). (c,d) Ratio of these velocities to that of the T2m median: (c) T2m,min, (d) T2m,max.